Nuclear-spin-dependent corrections to the transition polarizability in cesium

D. Xiao, H. B. Tran Tan, and A. Derevianko*
Department of Physics, University of Nevada, Reno, Nevada 89557, USA

(Received 9 July 2023; accepted 25 August 2023; published 6 September 2023)

The Stark-interference technique is commonly used to amplify the feeble parity-violating signal in atomic experiments. As a result, interpretation of these experiments in terms of electroweak observables requires knowledge of the Stark-induced $E1$ transition amplitudes or, equivalently, transition polarizabilities. While the literature assumes that these transition polarizabilities do not depend on the nuclear spin, here we prove the contrary. The nuclear-spin dependence arises due to the hyperfine mixing of atomic states and requires a third-order perturbation theory (one hyperfine interaction and two electric-dipole interactions) treatment. We demonstrate that the so far neglected *tensor* contribution appears in the transition polarizability and present numerical results for the nuclear-spin-dependent corrections to the $6S_{1/2} \to 7S_{1/2}$ transition polarizability in ^{133}Cs. We investigate the effect of these corrections to transition polarizabilities on the extraction of the ^{133}Cs anapole moment from the Boulder experiment [Science **275**, 1759 (1997)]. We also consider their effect on the extraction of the ratio between the scalar and vector transition polarizabilities from the measurements [Phys. Rev. A **55**, 1007 (1997)]. While the corrections are minor at the current level of experimental accuracy, our analysis provides a framework for future experiments.

DOI: 10.1103/PhysRevA.108.032805

I. INTRODUCTION

In 1988, an experiment performed by the Boulder group [1] provided the first evidence of the nuclear-spin-dependent parity-nonconserving (PNC) interactions in a ^{133}Cs atom, which later led to the discovery of the ^{133}Cs nuclear anapole moment [2]. However, the extracted nuclear anapole moment [2] has been found to disagree with the nuclear-physics determination [3]. In nuclear physics, to bridge different manifestations of PNC, theorists operate in terms of weak meson-nucleon couplings [4]. Weak meson-nucleon couplings propagate through the nuclear structure evaluation of anapole moments [3] and other nuclear processes. Linear combinations of these couplings can be constrained by comparison with available experimental data and theoretical estimates within the standard model framework. In particular, the nuclear-physics constraints come from the scattering of polarized protons on unpolarized protons and ^{4}He targets as well as the emission of circularly polarized photons from ^{18}F and ^{19}F nuclei. These constraints form nuclear experimental bands whose intersection yields the nuclear-physics determinations of the couplings. However, the bounds derived from the measured Cs anapole moment lie outside this nuclear-physics favored region. Our paper is motivated in part by this tension between the nuclear and atomic physics determinations of the weak meson-nucleon couplings.

The anapole moment is extracted from the difference between the two measured PNC amplitudes $E1_{\rm PNC}$ connecting different hyperfine components of the ground $6S_{1/2}$ and the excited $7S_{1/2}$ states in ^{133}Cs. The Boulder results read [2]

$$\frac{\mathrm{Im}(E1_{\rm PNC})}{\beta} = \begin{cases} -1.6349(80)\ \mathrm{mV/cm} \\ \quad \text{for } 6S_{1/2},\ F_i = 4 \to 7S_{1/2},\ F_f = 3, \\ -1.5576(77)\ \mathrm{mV/cm} \\ \quad \text{for } 6S_{1/2},\ F_i = 3 \to 7S_{1/2},\ F_f = 4. \end{cases} \tag{1}$$

Here, F is the grand total angular momentum in Cs formed by adding the nuclear spin $I = 7/2$ and the total electronic angular momentum J, and β is the vector transition polarizability. A weighted average of the two values in Eq. (1) yields the nuclear-spin-independent electroweak observable (weak charge), while their difference yields the nuclear-spin-dependent quantity (nuclear anapole moment).

Notice the appearance of the vector transition polarizability β in the results (1), as the Boulder group used the Stark-interference technique [5]. This technique amplifies the feeble PNC effect by the means of an externally applied dc electric field which opens an additional Stark-induced excitation pathway for the nominally $E1$-forbidden $6S_{1/2} \to 7S_{1/2}$ transition. Then the transition rate acquires a cross term between the Stark-induced and PNC amplitudes. This interference term flips sign under parity reversals enabling its experimental extraction.

One of the assumptions made in the Boulder analysis is that β does not depend on the nuclear spin. Contrary to this assumption, here we identify nuclear-spin-dependent corrections to the Stark-induced transition amplitudes or, equivalently, to the transition polarizabilities (β in particular). While the effects of our corrections turn out to be negligible

*andrei@unr.edu

at the Boulder experiment's level of accuracy, our analysis provides a framework for future experimental efforts.

The paper is organized as follows. In Sec. II, we review the Stark-interference technique and derive the second-order transition polarizabilities. The hyperfine-mediated corrections to the transition polarizabilities are derived in Sec. III and numerically evaluated in Sec. IV. Our reanalysis of the Boulder atomic parity violation (APV) experiment [2] is given in Sec. V A. We also compute a correction to the experimentally extracted ratio of the vector and scalar transition polarizabilities in Sec. V B. While we keep the discussion sufficiently general, all our numerical work refers to the $6S_{1/2} \to 7S_{1/2}$ transition in ^{133}Cs. Unless stated otherwise, atomic units are used throughout.

II. GENERALIZATION OF STARK-INDUCED TRANSITION POLARIZABILITY

We are interested in driving an electric-dipole transition from the an initial state i to a final state f. We assume that these states are of the same parity, precluding $E1$ transitions. To open the otherwise forbidden $E1$ pathway, we apply a dc electric field which admixes intermediate states of opposite parity into i and f [5]. The relevant amplitude for the resulting $E1$ transition between such mixed states can be derived in the second order of perturbation theory (see Ref. [6] for a detailed derivation). The two perturbations are the electric dipole interactions with the applied dc and driving laser fields. The Stark-induced transition amplitude $A_{i\to f}$ is conventionally expressed in terms of the transition polarizability $a_{i\to f}$ as $A_{i\to f} = a_{i\to f}\mathcal{E}_s\mathcal{E}_L$, which factors out $\mathcal{E}_s$ and $\mathcal{E}_L$, the static and laser field amplitudes, respectively. The transition polarizability for the transitions between two $S_{1/2}$ states is conventionally parametrized as [5]

$$a_{i\to f} = \alpha(\hat{\boldsymbol{\epsilon}}\cdot\hat{\boldsymbol{e}})\delta_{F_iF_f}\delta_{M_iM_f} + i\beta(\hat{\boldsymbol{e}}\times\hat{\boldsymbol{\epsilon}})\cdot\langle f|\boldsymbol{\sigma}|i\rangle. \quad (2)$$

Here, the two atomic-structure-dependent quantities α and β are the scalar and the vector transition polarizabilities. The unit vectors $\hat{\boldsymbol{\epsilon}}$ and $\hat{\boldsymbol{e}}$ characterize polarizations of the laser and static electric fields, respectively. The states i and f are hyperfine basis states, e.g., $|i\rangle = |n_i(IJ_i)F_iM_i\rangle$ is a state of grand total angular momentum F_i obtained by the conventional coupling of the total electron angular momentum J_i and the nuclear spin I_i, with M_i and n_i being the magnetic and principal quantum numbers. The matrix element of Pauli matrices $\boldsymbol{\sigma}$ is understood as involving the angular parts of the wave functions.

Qualitatively, Eq. (2) is obtained [6] in the second order of perturbation theory by recouping the product of two dipole couplings $(\boldsymbol{D}\cdot\hat{\boldsymbol{\epsilon}})(\boldsymbol{D}\cdot\hat{\boldsymbol{e}})$ into a sum over the irreducible tensor operators (ITOs) containing scalar products of compound tensors[1] $(\hat{\boldsymbol{\epsilon}}\otimes\hat{\boldsymbol{e}})^{(Q)}\cdot(\boldsymbol{D}\otimes\boldsymbol{D})^{(Q)}$. Here, $\boldsymbol{D}$ is the electron electric dipole moment operator. Based on the angular selection rules, the rank Q can accept the values of 0, 1, and 2, corresponding to the scalar, vector, and tensor contributions. Hereto, previous analyses of the $6S_{1/2} \to 7S_{1/2}$ transition polarizability in Cs have neglected the tensor ($Q = 2$) contribution. The reason for this is that the dipole operators involve only electronic degrees of freedom and the matrix element of the rank-2 tensor between the $S_{1/2}$ states vanishes due to the angular selection rules. However, if we account for the hyperfine interaction (HFI), the states involved would need to be characterized by the grand total angular momentum F and the tensor contribution would no longer vanish since $F = 3$ or 4 for the hyperfine manifolds attached to the $S_{1/2}$ electronic states in ^{133}Cs. Notice that the inclusion of the HFI requires a third-order perturbation theory treatment and therefore leads to the tensor contribution being suppressed compared to the scalar and vector contributions.

The tensor contribution to Eq. (2) can be parametrized as

$$a_{i\to f} = \cdots + \gamma\langle f|\{I\otimes I\}^{(2)}|i\rangle(\hat{\boldsymbol{\epsilon}}\otimes\hat{\boldsymbol{e}})^{(2)}, \quad (3)$$

where our tensor transition polarizability γ depends on both the nuclear and electronic structure. We have introduced an auxiliary rank-2 tensor $\{I\otimes I\}^{(2)}$ in front of the tensor polarizability to factor out the dependence on magnetic quantum numbers. Combined with this tensor term, Eq. (2) is the most general parametrization of the transition polarizability as long as we only keep interactions linear in the static and laser fields. It is worth noting that in the second order, due to a particular selection of prefactors in Eq. (2), α and β do not depend on the hyperfine components of the initial and final states. We will demonstrate that the HFI-mediated corrections would introduce the F_i and F_f dependence to the scalar and vector polarizabilities.

Based on these arguments, and taking into account the fact that the HFI is a scalar (see the discussion in Sec. III), we rewrite Eq. (2) in the following generalized form that now includes the tensor contribution (3), as well as the F dependence of the scalar and vector polarizabilities,

$$\begin{aligned} a_{i\to f} =& -\sqrt{3(2F_f+1)}w_0(\hat{\boldsymbol{\epsilon}},\hat{\boldsymbol{e}})\alpha^{F_i\to F_f}\delta_{F_iF_f}\delta_{M_iM_f} \\ & -\sqrt{2}\langle f||\sigma||i\rangle w_1(\hat{\boldsymbol{\epsilon}},\hat{\boldsymbol{e}})\beta^{F_i\to F_f} \\ & +\langle f||\{I\otimes I\}^{(2)}||i\rangle w_2(\hat{\boldsymbol{\epsilon}},\hat{\boldsymbol{e}})\gamma^{F_i\to F_f}, \end{aligned} \quad (4)$$

where we have used the Wigner-Eckart theorem and introduced the multipolar polarization weights [6]

$$\begin{aligned} w_Q(\hat{\boldsymbol{\epsilon}},\hat{\boldsymbol{e}}) =& (-1)^Q\sum_{M_Q}(-1)^{M_Q+F_f-M_f} \\ & \times\begin{pmatrix} F_f & Q & F_i \\ -M_f & -M_Q & M_i\end{pmatrix}(\hat{\boldsymbol{\epsilon}}\otimes\hat{\boldsymbol{e}})^{(Q)}_{M_Q}, \end{aligned} \quad (5)$$

with M_f, M_Q, and M_i being the magnetic quantum numbers. Note that selection rules fix the value of $M_Q = M_i - M_f$. The compound tensors of rank Q for the two vectors $\hat{\boldsymbol{\epsilon}}$ and $\hat{\boldsymbol{e}}$ are understood as $(\hat{\boldsymbol{\epsilon}}\otimes\hat{\boldsymbol{e}})^{(Q)}_{M_Q} = \sum_{\mu\nu}C^{QM_Q}_{1\mu1\nu}\hat{\epsilon}_\mu\hat{e}_\nu$, where $C^{QM_Q}_{1\mu1\nu}$ are Clebsch-Gordan coefficients and the A_μ components of a vector $\boldsymbol{A}$ in the spherical (or helicity) basis expressed in terms of its Cartesian components as [7] $A_0 = A_z$, $A_{+1} = -(A_x + iA_y)/\sqrt{2}$, $A_{-1} = (A_x - iA_y)/\sqrt{2}$. In particular, the

[1] A scalar product of two rank-k ITOs is understood as $P^{(k)}\cdot Q^{(k)} = \sum_{q=-k}^{k}(-1)^qP^{(k)}_qQ^{(k)}_{-q}$, and a compound ITO of rank Q is defined as $\{P^{(k_1)}\otimes R^{(k_2)}\}^{(Q)}_q = \sum_{q_1q_2}C^{Qq}_{k_1q_1k_2q_2}P^{(k_1)}_{q_1}R^{(k_2)}_{q_2}$, where q_1 and q_2 label the spherical basis components of the ITOs with $C^{Qq}_{k_1q_1k_2q_2}$ being the conventional Clebsch-Gordan coefficients.

combinations of polarization vectors are $(\hat{\boldsymbol{\varepsilon}} \otimes \hat{\boldsymbol{\varepsilon}})^{(0)} = -(\hat{\boldsymbol{\varepsilon}} \cdot \hat{\boldsymbol{\varepsilon}})/\sqrt{3}$ and $(\hat{\boldsymbol{\varepsilon}} \otimes \hat{\boldsymbol{\varepsilon}})^{(1)} = i(\hat{\boldsymbol{\varepsilon}} \times \hat{\boldsymbol{\varepsilon}})/\sqrt{2}$, in agreement with Eq. (2). We will consider the relevant components of the rank-2 tensor $(\hat{\boldsymbol{\varepsilon}} \otimes \hat{\boldsymbol{\varepsilon}})^{(2)}$ in Sec. V A.

Here, we note that the reduced matrix elements of the auxiliary rank-2 tensor $\{I \otimes I\}^{(2)}$ present in Eq. (4) is given by

$$\langle f||\{I \otimes I\}^{(2)}||i\rangle = (-1)^{2F_i - F_f + I - J_f}\sqrt{5}\,[F_f, F_i]^{1/2} \times I(I+1)[I]\begin{Bmatrix} 1 & 1 & 2 \\ I & I & I \end{Bmatrix}\delta_{J_i J_f}, \tag{6}$$

where $[J_1, J_2, \ldots, J_n] \equiv (2J_1 + 1)(2J_2 + 1)\cdots(2J_n + 1)$. For our target $6S_{1/2} \to 7S_{1/2}$ transition in ^{133}Cs, the above expression evaluates to

$$\langle F_f||\{I \otimes I\}^{(2)}||F_i\rangle = (-1)^{F_f} 6\sqrt{35}[F_f, F_i]^{1/2}, \tag{7}$$

which, for the special case where $F_{f,i} = 3, 4$, gives

$$\langle 3||\{I \otimes I\}^{(2)}||3\rangle = -42\sqrt{35}, \tag{8a}$$

$$\langle 4||\{I \otimes I\}^{(2)}||4\rangle = 54\sqrt{35}, \tag{8b}$$

$$\langle 3||\{I \otimes I\}^{(2)}||4\rangle = -126\sqrt{5}, \tag{8c}$$

$$\langle 4||\{I \otimes I\}^{(2)}||3\rangle = 126\sqrt{5}. \tag{8d}$$

We will need these values in our analysis for ^{133}Cs.

To reiterate, due to the HFI, the scalar, vector, and tensor transition polarizabilities entering Eq. (4) have an F dependence of the form ($X = \alpha, \beta, \gamma$)

$$X^{F_i \to F_f} = X^{[2]} + \delta X^{F_i \to F_f}, \tag{9}$$

where the second-order term $X^{[2]}$ is F independent. For the $S_{1/2} \to S_{1/2}$ transitions, $\gamma^{[2]} \equiv 0$, thereby $\gamma^{F_i \to F_f} = \delta\gamma^{F_i \to F_f}$. Expressions for the second-order scalar and vector transition polarizabilities, $\alpha^{[2]}$ and $\beta^{[2]}$, can be found, e.g., in Ref. [6]. Substantial attention [6,8–15] has been paid over the years to determining their accurate values since they are required for interpreting the results of APV experiments. As the reference values for the second-order polarizabilities for the $6S_{1/2} \to 7S_{1/2}$ transition in ^{133}Cs, we use values computed recently by our group [6],

$$\alpha^{[2]} = -266.31(23), \tag{10a}$$

$$\beta^{[2]} = 26.912(30), \tag{10b}$$

$$\gamma^{[2]} = 0. \tag{10c}$$

These values are in atomic units a_0^3, where a_0 is the Bohr radius.

We now proceed to the derivation of the hyperfine corrections $\delta\alpha^{F_i \to F_f}$, $\delta\beta^{F_i \to F_f}$, and $\delta\gamma^{F_i \to F_f}$ to transition polarizabilities.

III. HYPERFINE CORRECTIONS TO TRANSITION POLARIZABILITIES

To evaluate the hyperfine-mediated corrections to the transition polarizability, we follow the third-order formalism developed in Refs. [16–18]. References [16,17] computed the static differential polarizabilities for transitions between levels of the hyperfine manifold attached to the $S_{1/2}$ ground state.

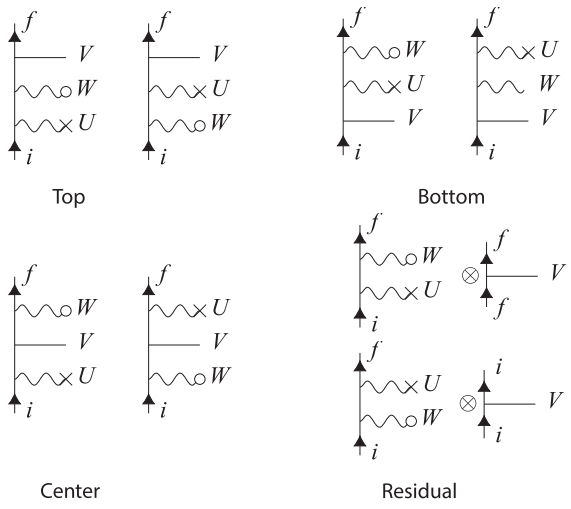

FIG. 1. Top, bottom, center, and residual (normalization) diagrams contributing to the hyperfine-mediated corrections to transition polarizability. Here, i and f denote the initial and the final states; W, U, and V represent the electric dipole $-\hat{\boldsymbol{\varepsilon}} \cdot \boldsymbol{D}$, $-\hat{\boldsymbol{\varepsilon}} \cdot \boldsymbol{D}$, and the hyperfine interaction $V^{\rm HFI}$, respectively.

Reference [18] generalized that formalism to the evaluation of dynamic (ac) polarizabilities. These papers focused on the characterization of clock shifts, which formally map into the evaluation of the diagonal matrix elements of the transition amplitude. Here, we further generalize our earlier formalism and consider *off-diagonal* matrix elements of the transition amplitude. In the context of APV, Ref. [19] has considered transition polarizabilities (including the tensor contribution) for transitions between hyperfine components attached to the Cs ground state.

The four relevant diagrams representing third-order contributions to the $i \to f$ transition amplitude, top (T), center (C), bottom (B), and residual (R), are shown in Fig. 1, with each diagram involving one hyperfine interaction and two $E1$ interactions (one with the laser, and another one with the static field). These diagrams are named after the position of the hyperfine interaction in the string of three operators. Explicitly, these terms read

$$T_{i\to f} = \sum_{ab} \frac{V^{\rm HFI}_{fa}(\hat{\boldsymbol{\varepsilon}} \cdot \boldsymbol{D}_{ab})(\hat{\boldsymbol{\varepsilon}} \cdot \boldsymbol{D}_{bi})}{\Delta E_{fa}\Delta E_{ib}} + \sum_{ab} \frac{V^{\rm HFI}_{fa}(\hat{\boldsymbol{\varepsilon}} \cdot \boldsymbol{D}_{ab})(\hat{\boldsymbol{\varepsilon}} \cdot \boldsymbol{D}_{bi})}{\Delta E_{fa}\Delta E_{fb}}, \tag{11a}$$

$$B_{i\to f} = \sum_{ab} \frac{(\hat{\boldsymbol{\varepsilon}} \cdot \boldsymbol{D}_{fa})(\hat{\boldsymbol{\varepsilon}} \cdot \boldsymbol{D}_{ab})V^{\rm HFI}_{bi}}{\Delta E_{ia}\Delta E_{ib}} + \sum_{ab} \frac{(\hat{\boldsymbol{\varepsilon}} \cdot \boldsymbol{D}_{fa})(\hat{\boldsymbol{\varepsilon}} \cdot \boldsymbol{D}_{ab})V^{\rm HFI}_{bi}}{\Delta E_{fa}\Delta E_{ib}}, \tag{11b}$$

$$C_{i\to f} = \sum_{ab} \frac{(\hat{\boldsymbol{\varepsilon}} \cdot \boldsymbol{D}_{fa})V^{\rm HFI}_{ab}(\hat{\boldsymbol{\varepsilon}} \cdot \boldsymbol{D}_{bi})}{\Delta E_{ia}\Delta E_{ib}} + \sum_{ab} \frac{(\hat{\boldsymbol{\varepsilon}} \cdot \boldsymbol{D}_{fa})V^{\rm HFI}_{ab}(\hat{\boldsymbol{\varepsilon}} \cdot \boldsymbol{D}_{bi})}{\Delta E_{fa}\Delta E_{fb}}, \tag{11c}$$

$$R_{i\to f} = -V_{ii}^{\rm HFI}\sum_a \frac{(\hat{\boldsymbol{\epsilon}}\cdot\boldsymbol{D}_{fa})(\hat{\boldsymbol{\epsilon}}\cdot\boldsymbol{D}_{ai})}{(\Delta E_{ia})^2} - V_{ff}^{\rm HFI}\sum_a \frac{(\hat{\boldsymbol{\epsilon}}\cdot\boldsymbol{D}_{fa})(\hat{\boldsymbol{\epsilon}}\cdot\boldsymbol{D}_{ai})}{(\Delta E_{fa})^2}, \tag{11d}$$

where $\Delta E_{ij} \equiv E_i - E_j$. Note that the two terms inside each combination differ by the swap of the two polarization vectors $\hat{\boldsymbol{\epsilon}}$ and $\hat{\boldsymbol{\epsilon}}$. Otherwise, the structure of the terms is similar. Further, the bottom and top diagrams are related as $B_{f\leftrightarrow i} = T^*_{i\leftrightarrow f}$.

Before carrying out the angular reduction of the expressions above, we briefly review the hyperfine interaction present in Eqs. (11a). Following the notation of Ref. [20], the interaction of electrons with nuclear multipolar moments may be expressed as

$$V^{\rm HFI} = \sum_N \mathcal{T}^{(N)}\cdot\mathcal{N}^{(N)}, \tag{12}$$

where the rank-N tensors $\mathcal{T}^{(N)}$ act in the electron space, and $\mathcal{N}^{(N)}$ act in the nuclear space. Note that $V^{\rm HFI}$ is a scalar ITO. The nuclear reduced matrix elements $\langle\gamma I||\mathcal{N}^{(N)}||\gamma I\rangle$ are expressed in terms of the conventional nuclear magnetic-dipole ($M1$) μ and electric-quadrupole ($E2$) Q moments as

$$\langle\gamma I||\mathcal{N}^{(1)}||\gamma I\rangle = \sqrt{\frac{(2I+1)(I+1)}{I}}\mu, \tag{13a}$$

$$\langle\gamma I||\mathcal{N}^{(2)}||\gamma I\rangle = \sqrt{\frac{(2I+1)(I+1)(2I+3)}{4I(2I-1)}}Q. \tag{13b}$$

Here, the magnetic-dipole moment $\mu \equiv g_I I\mu_N$ with μ_N being the nuclear magneton and g_I being the gyromagnetic ratio. For ^{133}Cs, $g_I = 0.737\,14$. As for the nuclear electric-quadrupole moment Q, the measured hyperfine constant B can be used to extract its value using theoretical values of the hyperfine electronic matrix elements. However, different measurements of B yield different determinations. For instance, the measured [21] hyperfine constant B in the ^{133}Cs $6P_{3/2}$ state is $-0.4934(17)$ MHz, which differs from a more recent result [22] of $-0.5266(57)$ MHz by about 7%. Because the uncertainty in B of Ref. [21] is smaller, we simply adopt the value $Q = -3.55(4)$ mb therefrom. Moreover, we find that the nuclear quadrupole contributions to the transition polarizabilities are suppressed compared to those due to the magnetic-dipole hyperfine interaction. For the same reason, we neglect even higher-rank nuclear multipoles, such as the poorly known magnetic octupole moment [21], due to their diminishing role as compared to the magnetic-dipole contribution.

To flesh out the tensorial structure of the transition polarizability resulting from the diagrams (11a), we use the same recoupling angular momentum algebra technique as in our derivation of the second-order expressions [6]. Since the HFI is a scalar ITO, the resulting tensorial structure of the transition polarizability is indeed given by Eq. (4). The hyperfine corrections to transition polarizabilities are therefore given by

$$\delta\alpha^{F_i\to F_f} = -\frac{\langle f||T^{(0)}+B^{(0)}+C^{(0)}+R^{(0)}||i\rangle}{\sqrt{3(2F_f+1)}}, \tag{14a}$$

$$\delta\beta^{F_i\to F_f} = -\frac{\langle f||T^{(1)}+B^{(1)}+C^{(1)}+R^{(1)}||i\rangle}{\sqrt{2}\langle f||\sigma||i\rangle}, \tag{14b}$$

$$\delta\gamma^{F_i\to F_f} = \frac{\langle f||T^{(2)}+B^{(2)}+C^{(2)}+R^{(2)}||i\rangle}{\langle f||\{I\otimes I\}^{(2)}||i\rangle}. \tag{14c}$$

We remind the reader that the various transition polarizabilities entering Eq. (4) are assembled as $X^{F_i\to F_f} = X^{[2]} + \delta X^{F_i\to F_f}$, where the second-order term $X^{[2]}$ is F independent. We listed our recommended values [6] for the second-order transition polarizabilities in Eqs. (10).

The reduced matrix elements of individual diagrams entering Eqs. (14) are given by

$$\langle f||T^{(Q)}||i\rangle = \sum_{NJ_aJ_b}(-1)^{F_f-F_i+J_a+J_i}[F_f,F_i,Q]^{1/2} \times\begin{Bmatrix} F_f & I & J_a\\ N & J_f & I\end{Bmatrix}\begin{Bmatrix} Q & J_i & J_a\\ I & F_f & F_i\end{Bmatrix}\begin{Bmatrix} Q & J_i & J_a\\ J_b & 1 & 1\end{Bmatrix} \times\left\{S_T^{(J_aJ_bN)}[fi] + (-1)^Q S_T^{(J_aJ_bN)}[ff]\right\}, \tag{15a}$$

$$\langle f||B^{(Q)}||i\rangle = \sum_{NJ_aJ_b}(-1)^{J_i+J_b}[F_f,F_i,Q]^{1/2} \times\begin{Bmatrix} F_i & I & J_b\\ N & J_i & I\end{Bmatrix}\begin{Bmatrix} Q & J_f & J_b\\ I & F_i & F_f\end{Bmatrix}\begin{Bmatrix} Q & J_b & J_f\\ J_a & 1 & 1\end{Bmatrix} \times\left\{S_B^{(J_aJ_bN)}[ii] + (-1)^Q S_B^{(J_aJ_bN)}[fi]\right\}, \tag{15b}$$

$$\langle f||C^{(Q)}||i\rangle = \sum_{NJ_aJ_b}(-1)^{J_a-J_i+F_i-F_f+N+1}[F_f,F_i,Q]^{1/2} \times\sum_j[j]\begin{Bmatrix} J_f & J_i & j\\ F_f & F_i & Q\\ I & I & N\end{Bmatrix}\begin{Bmatrix} J_f & J_i & j\\ 1 & 1 & Q\\ J_a & J_b & N\end{Bmatrix} \times\left\{S_C^{(J_aJ_bN)}[ii] + (-1)^Q S_C^{(J_aJ_bN)}[ff]\right\}, \tag{15c}$$

$$\langle f||R^{(Q)}||i\rangle = (-1)^{2F_f-I+F_i+J_i+1}[F_f,F_i,Q]^{1/2} \times\begin{Bmatrix} Q & J_f & J_i\\ I & F_i & F_f\end{Bmatrix}\sum_{J_a}\begin{Bmatrix} Q & J_i & J_f\\ J_a & 1 & 1\end{Bmatrix} \times\left\{V[i]S_R^{J_a}[f] + (-1)^Q V[f]S_R^{J_a}[i]\right\}, \tag{15d}$$

which are expressed in terms of the reduced sums

$$S_T^{(J_aJ_bN)}[\alpha\beta] = \sum_{n_an_b}\frac{\langle I||\mathcal{N}^{(N)}||I\rangle\langle n_fJ_f||\mathcal{T}^{(N)}||n_aJ_a\rangle\langle n_aJ_a||D||n_bJ_b\rangle\langle n_bJ_b||D||n_iJ_i\rangle}{\Delta E_{\alpha a}\Delta E_{\beta b}}, \tag{16a}$$

$$S_B^{(J_aJ_bN)}[\alpha\beta] = \sum_{n_an_b}\frac{\langle n_fJ_f||D||n_aJ_a\rangle\langle n_aJ_a||D||n_bJ_b\rangle\langle I||\mathcal{N}^{(N)}||I\rangle\langle n_bJ_b||\mathcal{T}^{(N)}||n_iJ_i\rangle}{\Delta E_{\alpha a}\Delta E_{\beta b}}, \tag{16b}$$

$$S_C^{(J_a J_b N)}[\alpha\beta] = \sum_{n_a n_b} \frac{\langle n_f J_f||D||n_a J_a\rangle\langle I||\mathcal{N}^{(N)}||I\rangle\langle n_a J_a||\mathcal{T}^{(N)}||n_b J_b\rangle\langle n_b J_b||D||n_i J_i\rangle}{\Delta E_{\alpha a}\Delta E_{\beta b}}, \tag{16c}$$

$$S_R^{(J_a)}[\alpha] = \sum_{n_a} \frac{\langle n_f J_f||D||n_a J_a\rangle\langle n_a J_a||D||n_i J_i\rangle}{(\Delta E_{\alpha a})^2}, \tag{16d}$$

and the HFI diagonal matrix elements

$$V[\alpha] = (-1)^{I+J_\alpha+F_\alpha}\sum_N \begin{Bmatrix} F_\alpha & J_\alpha & I \\ N & I & J_\alpha \end{Bmatrix} \times \langle n_\alpha J_\alpha||\mathcal{T}^{(N)}||n_\alpha J_\alpha\rangle\langle I||\mathcal{N}^{(N)}||I\rangle. \tag{17}$$

IV. NUMERICAL RESULTS FOR HYPERFINE CORRECTIONS

In Sec. III, we have presented the formulation for the hyperfine corrections to the scalar, vector, and tensor transition polarizabilities. In this section, we present our numerical results, which are compiled in Table I. To arrive at these values, we employed relativistic many-body methods for computing the atomic structure. A detailed discussion of these methods and their numerical implementation can be found in Refs. [6,23] and references therein. Simply put, we used the frozen-core V^{N-1} Dirac-Hartree-Fock (DHF), Brueckner orbitals (BOs), and random phase approximation (RPA). Among these approximations the RPA(BO) approach is the most complete as it incorporates the core polarization and the core screening effects. The RPA(BO) results are listed in Table I. In our calculations, we use a dual-kinetic balance B-spline DHF basis set [24] containing $N = 60$ basis functions of order $k = 9$ per partial wave generated in a cavity of radius $R_{\rm max} = 250$ a.u., the same as in Refs. [6,23].

To improve the accuracy of our calculations, we also employ a semiempirical approach. To this end, we point out that there are three atomic properties entering the reduced sums: the energies, the $E1$ matrix elements, and the HFI matrix elements. We therefore replace a certain subset of *ab initio* RPA(BO) quantities with the experimental or other high-accuracy values. Determining this subset, however, requires some care. Indeed, although the low-n orbitals from the finite basis set closely resemble those obtained with the conventional finite-difference technique computed with practically infinite cavity radius, as n increases, the mapping of the basis states to physical states deteriorates. In our basis set, we find the boundary for the transition from physical to nonphysical orbitals to be at the radial quantum number $n_r = 12$, without loss of numerical accuracy for matrix elements and energies. Because of this, while evaluating the reduced sums, we use the National Institute of Science and Technology (NIST) recommended [25] energies for the physical states, $n_{a,b}P_J$ with $n_{a,b} = 6$–12 and $n_{a,b}D_J$ with $n_{a,b} = 5$–11. For the same reasons, we replace the RPA(BO) $E1$ matrix elements for the $6S_{1/2} \to n_{a,b}P_J$ and $7S_{1/2} \to n_{a,b}P_J$ channels with their experimental values tabulated in Ref. [12] for $n_{a,b} = 6, 7$ and with their high-accuracy relativistic coupled-cluster counterparts [23] for $n_{a,b} = 8$–12. For later discussion, contributions to the polarizabilities involving states $n_{a,b}P_J$ with $n_{a,b} = 6$–12 and $n_{a,b}D_J$ with $n_{a,b} = 5$–11 are called "main" terms, those with $n_{a,b}$ below these ranges are call "core-valence" (cv) terms, and those with $n_{a,b}$ above these ranges are call "tail" terms.

The semiempirical matrix elements of the hyperfine interaction involve "physical" states with principle quantum numbers $6 \leqslant n_{a,b} \leqslant 12$. We evaluate them as follows. The diagonal hyperfine matrix elements are extracted from the experimental values [26–28] of hyperfine constants A from the relation

$$A = \langle\mathcal{T}^{(1)}\rangle_J\langle\mathcal{N}^{(1)}\rangle_I/(IJ), \tag{18}$$

where $\langle\mathcal{T}^{(1)}\rangle_J$ and $\langle\mathcal{N}^{(1)}\rangle_I$ are the so-called stretched matrix elements expressed in terms of the reduced matrix elements

$$\langle\mathcal{O}^{(N)}\rangle_J = \begin{pmatrix} J & N & J \\ -J & 0 & J \end{pmatrix}\langle\gamma J||\mathcal{O}^{(N)}||\gamma J\rangle. \tag{19}$$

The off-diagonal HFI matrix elements between the $S_{1/2}$ states were evaluated as the geometric mean of the diagonal matrix elements [14]

$$\langle n'S_{1/2}|V^{\rm HFI}|nS_{1/2}\rangle = \langle n'S_{1/2}|V^{\rm HFI}|n'S_{1/2}\rangle^{1/2} \times \langle nS_{1/2}|V^{\rm HFI}|nS_{1/2}\rangle^{1/2}, \tag{20}$$

where the diagonal matrix elements come from the experimental values of the hyperfine constant A. The high accuracy of this approximation has been confirmed in Ref. [29]. The remaining off-diagonal magnetic-dipole HFS matrix elements between the "physical" states were determined using the relativistic coupled-cluster method, with the code described in Ref. [23]. As for the nuclear quadrupole HFI contributions, we

TABLE I. Hyperfine corrections to the scalar, $\delta\alpha^{F_i\to F_f}$, vector, $\delta\beta^{F_i\to F_f}$, and tensor, $\delta\gamma^{F_i\to F_f} = \gamma^{F_i\to F_f}$, transition polarizabilities for the indicated transitions in ^{133}Cs. Semiempirical values are anticipated to have better accuracy than the RPA(BO) results. The notation $x[y]$ stands for $x \times 10^y$.

Transition		RPA(BO)	Semiemp.
	$\delta\alpha$	−6.779[−3]	−7.315[−3]
$6S_{1/2}\,F=3 \to 7S_{1/2}\,F=3$	$\delta\beta$	2.681[−3]	2.735[−3]
	$\delta\gamma$	−1.209[−5]	−1.145[−5]
	$\delta\alpha$	0	0
$6S_{1/2}\,F=4 \to 7S_{1/2}\,F=3$	$\delta\beta$	−1.978[−4]	−1.272[−4]
	$\delta\gamma$	−1.849[−5]	−1.748[−5]
	$\delta\alpha$	0	0
$6S_{1/2}\,F=3 \to 7S_{1/2}\,F=4$	$\delta\beta$	7.937[−4]	7.351[−4]
	$\delta\gamma$	−1.849[−5]	−1.748[−5]
	$\delta\alpha$	5.273[−3]	5.689[−3]
$6S_{1/2}\,F=4 \to 7S_{1/2}\,F=4$	$\delta\beta$	−2.086[−3]	−2.127[−3]
	$\delta\gamma$	−1.804[−5]	−1.706[−5]

found them to be suppressed. Thereby, we kept their RPA(BO) matrix elements.

Our numerical results for the hyperfine corrections to transition polarizabilities are listed in Table I. Overall, the corrections to the polarizabilities are below the 10^{-2} a.u. level. The $\delta\alpha$ corrections are identically zero for the $F_i \neq F_f$ transitions due to the scalar nature of the underlying ITO. Otherwise, $|\delta\alpha^{F_i\to F_f}| \sim 5\times 10^{-3}$ is about five orders of magnitude smaller than $|\alpha^{[2]}| \approx 3\times 10^2$. As for the vector transition polarizability, $|\delta\beta^{F_i\to F_f}|$ is about four to five orders of magnitude smaller than $|\beta^{[2]}| \approx 3\times 10^1$. The $|\delta\beta^{F_i\to F_f}|$ corrections to the $F_i = F_f$ transitions are an order of magnitude larger than those for the $F_i \neq F_f$ transitions. We observe that the tensor transition polarizability, $\gamma^{F_i\to F_f} = \delta\gamma^{F_i\to F_f}$, is in the order of 10^{-5} a.u. The relative smallness of the numerical values of the tensor transition polarizabilities as compared to their scalar and vector counterparts is due, in part, to the large values, $\sim 3\times 10^2$, of the prefactors $\langle F_f||\{I\otimes I\}^{(2)}||F_i\rangle$ in Eq. (8). Further, $\gamma^{3\to 4} = \gamma^{4\to 3}$ as can be proven by a direct examination of our analytical expressions.

The difference between our RPA(BO) and semiempirical results for the main terms does not exceed 10%. We take this as a conservative estimate for the uncertainty in these contributions. To estimate the numerical uncertainties in cv and tail terms, we studied their convergence pattern with respect to the number N of basis functions. We find that at the DHF level the values of $\delta\alpha$ are affected at the level of $\lesssim$0.1% when varying N from 40 to 100, introducing negligible errors in the final values. The quantities $\delta\beta$ and $\delta\gamma$ are similarly affected.

V. DISCUSSION

We have presented the theoretical formulation and numerical estimate for the hyperfine corrections to the transition polarizabilities. In this section, we investigate the impact of neglecting the hyperfine-mediated tensor polarizability γ and the hyperfine-state dependence of the scalar α, and vector β polarizabilities on the extraction of electroweak observables from APV experiments. In particular, we reanalyze two Boulder experiments [2,30] and compute corrections to their extracted value of the ^{133}Cs anapole moment and the ratio α/β of the scalar and vector transition polarizabilities.

A. Reinterpretation of the Boulder parity violation measurement

We start by reviewing the Boulder APV experiment [2,31] and the assumptions that went into its analysis. The experiment utilized the Stark-interference technique to extract the ratio of the PNC amplitude to the vector transition polarizability, $\mathrm{Im}(E1_{\mathrm{PNC}})/\beta$. Notice the use of β without specifying hyperfine components, as the hyperfine corrections were neglected. It is our goal to introduce F-dependent corrections to β here.

The Boulder experiment used a spin-polarized ^{133}Cs beam subjected to a uniform and static electric field, with a laser driving the nominally $E1$-forbidden transition between various hyperfine components of the ground $6S_{1/2}$ and the excited $7S_{1/2}$ state. The dc electric field opens up an $E1$ transition channel between these states by mixing the S and P states. The total transition rate R is determined by a combination of the Stark-induced, parity-violating (PNC), and $M1$ transition amplitudes

$$R = \left|A^{\mathrm{Stark}}_{i\to f} + A^{\mathrm{PNC}}_{i\to f} + A^{M_1}_{i\to f}\right|^2, \tag{21}$$

where [31]

$$A^{\mathrm{Stark}}_{i\to f} = \alpha\boldsymbol{\mathcal{E}}_L\cdot\boldsymbol{\mathcal{E}}_S\,\delta_{F_fF_i}\delta_{M_fM_i} + i\beta(\boldsymbol{\mathcal{E}}_S\times\boldsymbol{\mathcal{E}}_L)\cdot\langle f|\boldsymbol{\sigma}|i\rangle, \tag{22a}$$

$$A^{\mathrm{PNC}}_{i\to f} = i\,\mathrm{Im}(E1_{\mathrm{PNC}})\boldsymbol{\mathcal{E}}_S\cdot\langle f|\boldsymbol{\sigma}|i\rangle, \tag{22b}$$

$$A^{M1}_{i\to f} = (M1)_{\mathrm{rad}}(\hat{\boldsymbol{k}}_L\times\boldsymbol{\mathcal{E}}_S)\cdot\langle f|\boldsymbol{\sigma}|i\rangle. \tag{22c}$$

Here, we have changed the notation of Ref. [31] to be consistent with that of the previous sections.

In Eqs. (22), $\boldsymbol{\mathcal{E}}_L = \mathcal{E}_L\hat{\boldsymbol{\epsilon}}$ is the laser field driving the transition with $\hat{\boldsymbol{k}}_L$ being a unit vector in its propagation direction, $\boldsymbol{\mathcal{E}}_S = \mathcal{E}_S\hat{\boldsymbol{e}}$ is the dc electric field, and α and β are the scalar and vector transition polarizabilities, introduced in earlier sections. To set the stage, for now, as in Ref. [31], we neglected the F dependence of α and β and omitted the tensor (γ) contribution. The PNC amplitude $E1_{\mathrm{PNC}}$ includes both the nuclear-spin-dependent and spin-independent effects and $(M1)_{\mathrm{rad}}$ stands for the radial integral of the $6S_{1/2}$-$7S_{1/2}$ $M1$ matrix element [31]. We will neglect the $A^{M1}_{i\to f}$ $M1$ amplitude for reasons discussed in Ref. [31].

The Stark-interference technique amplifies the feeble PNC amplitude $A^{\mathrm{PNC}}_{i\to f}$ with the help of the much stronger $A^{\mathrm{Stark}}_{i\to f}$ amplitude: The interference between $A^{\mathrm{PNC}}_{i\to f}$ and $A^{\mathrm{Stark}}_{i\to f}$ manifests itself as a cross term when expanding the square in the rate expression Eq. (21). To access this Stark-PNC interference term, the experiment [31] involved measuring the change in the transition rate R, Eq. (21), under various parity reversals, which included flipping the direction of the applied dc electric field, flipping the sign of the relevant component of the laser polarization, or changing the sign of the magnetic quantum numbers [31]. The PNC amplitude was extracted from two transition rates R^+ and R^- measured under opposite parities. A parity reversal results in a sign flip of the PNC amplitude $A^{\mathrm{PNC}}_{i\to f}$, while leaving the sign of the Stark-induced amplitude $A^{\mathrm{Stark}}_{i\to f}$ unaffected.

The Stark-induced amplitude $A^{\mathrm{Stark}}_{i\to f}$ in Eq. (22a) generally depends on both the scalar and vector polarizabilities. However, in the Boulder experiment, the transitions were driven between the states of different values of F ($F_i \neq F_f$), and thereby only the vector polarizability contribution remained in Eq. (22a). Therefore, it is the vector polarizability β that enters the interference term with $E1_{\mathrm{PNC}}$. Explicitly, the PNC amplitude was extracted from the normalized difference in the two transition rates,

$$\frac{R^+ - R^-}{R^+ + R^-} \propto \frac{\mathrm{Im}(E1_{\mathrm{PNC}})}{\beta}. \tag{23}$$

Next, we specify the geometry of the Boulder experiment [2,31]. In the setup of the Boulder experiment, a ^{133}Cs atomic beam travels along the z axis and an externally applied magnetic field is aligned along the beam propagation direction, defining the quantization axis. Before entering the excitation-laser interaction region, the Cs atoms are optically pumped into the "stretched" hyperfine sublevels of the $6S_{1/2}$

ground states, either $F_i = 3$, $M_i = \pm 3$ or $F_i = 4$, $M_f = \pm 4$. The transitions to the $7S_{1/2}$ hyperfine manifold are driven by a standing-wave laser with the cavity axis aligned along the y axis. The excitation laser field $\boldsymbol{\mathcal{E}}_L$ is elliptically polarized, $\boldsymbol{\mathcal{E}}_L = \mathcal{E}_L^z \hat{\mathbf{z}} + i\mathcal{E}_L^I \hat{\mathbf{x}}$. Finally, a static and uniform electric field $\boldsymbol{\mathcal{E}}_S = \mathcal{E}_S^x \hat{\mathbf{x}}$ is aligned along the x axis.

Having reviewed the Boulder experiment, now we examine the effect of our tensor transition polarizability γ, as well as the nuclear-spin-dependent corrections to α and β, and assess whether they affect the extraction of the PNC amplitude $E1_{\rm PNC}$. To this end, we rewrite Eq. (4) as

$$\begin{aligned} A_{i\to f}^{\rm Stark} =& \alpha^{F_i\to F_f} \boldsymbol{\mathcal{E}}_L \cdot \boldsymbol{\mathcal{E}}_S \delta_{F_f F_i} \delta_{M_f M_i} \\ &+ i\beta^{F_i\to F_f} (\boldsymbol{\mathcal{E}}_L \times \boldsymbol{\mathcal{E}}_S) \cdot \langle f|\boldsymbol{\sigma}|i\rangle \\ &+ \gamma^{F_i\to F_f} w_2(\hat{\boldsymbol{\varepsilon}}, \hat{\boldsymbol{e}}) \mathcal{E}_L \mathcal{E}_S \langle f||\{I\otimes I\}^{(2)}||i\rangle, \end{aligned} \tag{24}$$

where we have again used $A_{i\to f}^{\rm Stark} = \mathcal{E}_L \mathcal{E}_S\, a_{i\to f}$. The reduced matrix element $\langle f||\{I\otimes I\}^{(2)}||i\rangle$ is again given by Eq. (6) and the polarization and state-dependent factor is explicitly [cf. Eq. (5)]

$$\begin{aligned} w_2(\hat{\boldsymbol{\varepsilon}}, \hat{\boldsymbol{e}}) =& \sum_{M_Q=-2}^{2} (-1)^{M_Q+F_f-M_f} \\ &\times \begin{pmatrix} F_f & 2 & F_i \\ -M_f & -M_Q & M_i \end{pmatrix} (\hat{\boldsymbol{\varepsilon}} \otimes \hat{\boldsymbol{e}})^{(2)}_{M_Q}. \end{aligned} \tag{25}$$

The components of the rank-two compound tensor of electric field polarizations are

$$(\hat{\boldsymbol{\varepsilon}} \otimes \hat{\boldsymbol{e}})^{(2)}_{M_Q} = \sum_{\mu,\lambda=-1}^{1} C^{2M_Q}_{1\mu 1\lambda} \hat{\boldsymbol{\varepsilon}}_\mu \hat{\boldsymbol{e}}_\lambda. \tag{26}$$

Note that the selection rules for the $3j$-symbol fix $M_Q = M_i - M_f$ in Eq. (25). Moreover, since we are interested in transitions between stretched hyperfine states $|F, M_F = \pm F\rangle$ with $F_i = F_f \pm 1$, only terms with $M_Q = \pm 1$ survive in Eq. (25). For the Boulder experiment where $\hat{\boldsymbol{\varepsilon}} = \varepsilon_L^z \hat{\mathbf{z}} + i\varepsilon_L^I \hat{\mathbf{x}}$ and $\hat{\boldsymbol{e}} = \hat{\mathbf{x}}$, we find the needed components of the second-rank tensor to be $(\hat{\boldsymbol{\varepsilon}} \otimes \hat{\boldsymbol{e}})^{(2)}_{\pm 1} = \mp \frac{1}{2} \varepsilon_L^z$. Then the Stark-induced amplitude for transitions between stretched states with $F_i = F_f \pm 1$ can be simplified to

$$A_{i\to f}^{\rm Stark} = \beta^{F_i\to F_f} \mathcal{E}_L^z \mathcal{E}_S^x C^{F_f M_f}_{F_i M_f \pm 1} \pm \gamma^{F_i\to F_f} \mathcal{E}_L^z \mathcal{E}_S^x U^{F_f M_f}_{F_i M_f \pm 1}/2, \tag{27}$$

where $\mathcal{E}_L^z$ and $\mathcal{E}_S^x$ are the components of the laser and the applied dc electric fields, respectively. The coefficients $C^{F_f M_f}_{F_i M_f \pm 1}$ are defined as

$$\begin{aligned} C^{F_f M_f}_{F_i M_f \pm 1} =& \frac{(-1)^{I+S+F_i+1}}{2\sqrt{3}} [F_f, F_i]^{1/2} \begin{Bmatrix} 1/2 & F_f & I \\ F_i & 1/2 & 1 \end{Bmatrix} \\ &\times \begin{pmatrix} F_f & 1 & F_i \\ -M_f & \mp 1 & M_f \pm 1 \end{pmatrix}, \end{aligned} \tag{28}$$

and are tabulated in Ref. [32]. Here we introduced a similar coefficient,

$$\begin{aligned} U^{F_f M_f}_{F_i M_f \pm 1} =& (-1)^{F_f - M_f} \begin{pmatrix} F_f & 2 & F_i \\ -M_f & \mp 1 & M_f \pm 1 \end{pmatrix} \\ &\times \langle F_f||\{I\otimes I\}^{(2)}||F_i\rangle, \end{aligned} \tag{29}$$

which specifies the dependence of the tensor contribution on the magnetic quantum numbers. The "±" signs appearing in the $C^{F_f M_f}_{F_i M_f \pm 1}$ and $U^{F_f M_f}_{F_i M_f \pm 1}$ factors indicate the values of the magnetic quantum numbers for the initial state, given a fixed final state value of M_f. The "±" sign preceding the γ term originates from the rank-two compound tensor of the electric fields $(\hat{\boldsymbol{\varepsilon}} \otimes \hat{\boldsymbol{e}})^{(2)}_{M_Q}$ when the value of M_Q is changed from $+1$ to -1.

The values of the angular factors $C^{F_f M_f}_{F_i M_f \pm 1}$ and $U^{F_f M_f}_{F_i M_f \pm 1}$ relevant to our computation are explicitly

$$C^{4-4}_{3-3} = C^{44}_{33} = -C^{33}_{44} = -C^{3-3}_{4-4} = \sqrt{7/8}, \tag{30a}$$

$$U^{4-4}_{3-3} = -U^{44}_{33} = U^{33}_{44} = -U^{3-3}_{4-4} = -42\sqrt{3}. \tag{30b}$$

It is clear that these factors satisfy the following identities,

$$C^{F_f M_f}_{F_i M_f \pm 1} = C^{F_f - M_f}_{F_i - M_f \mp 1}, \tag{31a}$$

$$U^{F_f M_f}_{F_i M_f \pm 1} = -U^{F_f - M_f}_{F_i - M_f \mp 1}. \tag{31b}$$

The measured quantities [31] are the transition rates $R^{\pm}$, Eqs. (21), whose computation involves squaring out the sum of the Stark and PNC transition amplitudes. Our generalized Stark-induced amplitude is given by Eq. (27). The simplified PNC (22b) amplitude reads [31]

$$A_{i\to f}^{\rm PNC} = \mp {\rm Im}(E1_{\rm PNC}) \mathcal{E}_L^I C^{F_f M_f}_{F_i M_f \pm 1} \delta_{M_i, M_f \pm 1}. \tag{32}$$

Note that while $A_{i\to f}^{\rm Stark}$ depends on the z component of the laser field, $A_{i\to f}^{\rm PNC}$ depends on $\mathcal{E}_L^I = |\mathcal{E}_L^x|$. Then the generalized rates R^+ and R^- for the two transitions of opposite handedness are given by

$$\begin{aligned} R^+ \equiv& R(F_i, M_f - 1 \to F_f, M_f) \\ =& \beta^2 \left(\mathcal{E}_S^x \mathcal{E}_L^z\right)^2 \left(C^{F_f M_f}_{F_i M_f - 1}\right)^2 \\ &- \beta\gamma \mathcal{E}_S^x \mathcal{E}_L^{z\,2} C^{F_f M_f}_{F_i M_f - 1} U^{F_f M_f}_{F_i M_f - 1} \\ &+ 2\beta\, {\rm Im}(E1_{\rm PNC}) \mathcal{E}_S^x \mathcal{E}_L^z \mathcal{E}_L^I \left(C^{F_f M_f}_{F_i M_f - 1}\right)^2 \\ &- \gamma \mathcal{E}_L^z \mathcal{E}_S^x \mathcal{E}_L^I\, {\rm Im}(E1_{\rm PNC}) C^{F_f M_f}_{F_i M_f - 1} U^{F_f M_f}_{F_i M_f - 1}, \end{aligned} \tag{33a}$$

$$\begin{aligned} R^- \equiv& R(F_i, M_f + 1 \to F_f, M_f) \\ =& \beta^2 \left(\mathcal{E}_S^x \mathcal{E}_L^z\right)^2 \left(C^{F_f M_f}_{F_i M_f + 1}\right)^2 \\ &+ \beta\gamma \left(\mathcal{E}_S^x \mathcal{E}_L^z\right)^2 C^{F_f M_f}_{F_i M_f + 1} U^{F_f M_f}_{F_i M_f + 1} \\ &- 2\beta\, {\rm Im}(E1_{\rm PNC}) \mathcal{E}_S^x \mathcal{E}_L^z \mathcal{E}_L^I \left(C^{F_f M_f}_{F_i M_f + 1}\right)^2 \\ &- \gamma \mathcal{E}_L^z \mathcal{E}_S^x \mathcal{E}_L^I\, {\rm Im}(E1_{\rm PNC}) C^{F_f M_f}_{F_i M_f + 1} U^{F_f M_f}_{F_i M_f + 1}. \end{aligned} \tag{33b}$$

In the above expressions, F_i and F_f remain fixed in $R^{\pm}$, while the sign of M_f flips when going from Eq. (33a) to Eq. (33b). We remind the reader that we focus on the transitions between stretched hyperfine states. For example, for the $|3, 3\rangle \to |4, 4\rangle$ transition[2] one would use the R^+ expression, while the matching transition of opposite handedness would be $|3, -3\rangle \to$

[2]Here, we used the abbreviation $|F_i, M_i\rangle \to |F_f, M_f\rangle$, suppressing the electronic term parts of the wave functions.

$|4,-4\rangle$ with the R^- expression to be used. We will distinguish between four transition rates $R^+_{3\to4}$, $R^-_{3\to4}$, $R^+_{4\to3}$, and $R^-_{4\to3}$ referring to the transitions $|3,3\rangle \to |4,4\rangle$, $|3,-3\rangle \to |4,-4\rangle$, $|4,-4\rangle \to |3,-3\rangle$, and $|4,4\rangle \to |3,3\rangle$, respectively. For the sake of clarity, we have also suppressed the $F_i \to F_f$ superscripts in various polarizabilities.

Following Ref. [31], we are interested in the rate ratio

$$r_{F_i\to F_f} \equiv \left(\frac{R^+ - R^-}{R^+ + R^-}\right)_{F_i\to F_f} \tag{34}$$

as it separates out the PNC amplitude. With the help of Eq. (33) and the identities (31), the rate ratio generalizes to

$$r_{F_i\to F_f} = \frac{1 + \frac{\gamma^{F_i\to F_f}}{2\beta^{F_i\to F_f}} \frac{U^{F_f M_f}_{F_i M_f+1}}{C^{F_f M_f}_{F_i M_f+1}}}{1 + \frac{\gamma^{F_i\to F_f}}{\beta^{F_i\to F_f}} \frac{U^{F_f M_f}_{F_i M_f+1}}{C^{F_f M_f}_{F_i M_f+1}}} \frac{2\,\mathrm{Im}\big(E1^{F_i\to F_f}_{\mathrm{PNC}}\big)\mathcal{E}^I_L}{\beta^{F_i\to F_f}\mathcal{E}^z_L\mathcal{E}^x_S}, \tag{35}$$

where we have emphasized the nuclear-spin dependence of the PNC amplitude by reintroducing the $F_i \to F_f$ superscript into β and γ. In the limit of vanishing tensor polarizabilities $\gamma^{F_i\to F_f}$ and β being independent of F_i and F_f, Eq. (35) reproduces the Boulder experiment's expression [2,31]

$$r^{\mathrm{Boulder}}_{F_i\to F_f} = \frac{2\,\mathrm{Im}\big(E1^{F_i\to F_f}_{\mathrm{PNC}}\big)\mathcal{E}^I_L}{\beta^{[2]}\mathcal{E}^z_L\mathcal{E}^x_S}. \tag{36}$$

From Eq. (35), the ratios $r_{F_i\to F_f}$ for the $F_i = 3 \to F_f = 4$ and $F_i = 4 \to F_f = 3$ transitions are explicitly

$$r_{3\to4} = \frac{2 - 12\sqrt{42}\frac{\gamma^{3\to4}}{\beta^{3\to4}}}{1 - 12\sqrt{42}\frac{\gamma^{3\to4}}{\beta^{3\to4}}} \frac{\mathrm{Im}\big(E1^{3\to4}_{\mathrm{PNC}}\big)\mathcal{E}^I_L}{\beta^{3\to4}\mathcal{E}^z_L\mathcal{E}^x_S}, \tag{37a}$$

$$r_{4\to3} = \frac{2 + 12\sqrt{42}\frac{\gamma^{4\to3}}{\beta^{4\to3}}}{1 + 12\sqrt{42}\frac{\gamma^{4\to3}}{\beta^{4\to3}}} \frac{\mathrm{Im}\big(E1^{4\to3}_{\mathrm{PNC}}\big)\mathcal{E}^I_L}{\beta^{4\to3}\mathcal{E}^z_L\mathcal{E}^x_S}, \tag{37b}$$

which can be further simplified to

$$r_{3\to4} \approx r^{\mathrm{Boulder}}_{3\to4}\left(1 - \frac{\delta\beta^{3\to4}}{\beta^{[2]}} + 6\sqrt{42}\frac{\gamma^{3\to4}}{\beta^{[2]}}\right), \tag{38a}$$

$$r_{4\to3} \approx r^{\mathrm{Boulder}}_{4\to3}\left(1 - \frac{\delta\beta^{4\to3}}{\beta^{[2]}} - 6\sqrt{42}\frac{\gamma^{4\to3}}{\beta^{[2]}}\right), \tag{38b}$$

where the last two terms in the parenthesis are the F-dependent corrections to the Boulder expressions. With our results from Table I, the corrections evaluate to -5×10^{-5} and 3×10^{-5} for the $3\to4$ and the $4\to3$ transitions, respectively. These are smaller than the experimental uncertainties in the $\mathrm{Im}(E1^{F_i\to F_f}_{\mathrm{PNC}})$ determination.

The PNC amplitudes $E1_{\mathrm{PNC}}$ include both the nuclear-spin-independent and nuclear-spin-dependent contributions. The largest impact of our analysis is on the extraction of the nuclear-spin-dependent part (which includes the anapole moment contribution). If we neglect the hyperfine corrections to the transition polarizabilities, the anapole moment contribution is extracted as [31]

$$\frac{\mathrm{Im}\big(E1^{\mathrm{anapole}}_{\mathrm{PNC}}\big)^{\mathrm{Boulder}}}{\beta^{[2]}} = \big(r^{\mathrm{Boulder}}_{3\to4} - r^{\mathrm{Boulder}}_{4\to3}\big)\frac{\mathcal{E}^x_S\mathcal{E}^z_L}{2\mathcal{E}^I_L}, \tag{39}$$

where the authors of Ref. [31] associated the measured rates with $r^{\mathrm{Boulder}}_{F_i\to F_f}$. The measured rates $r_{F_i\to F_f}$ are, however, more accurately given as in Eq. (35).

To account for the nuclear-spin-dependent effects on transition polarizabilities, we thus reexpress $r^{\mathrm{Boulder}}_{3\to4}$ and $r^{\mathrm{Boulder}}_{4\to3}$ in terms of $r_{3\to4}$ and $r_{4\to3}$ using Eqs. (38) and use these "adjusted" Boulder rates in Eq. (39). With our semiempirical values from Table I, we find $r^{\mathrm{Boulder}}_{3\to4} = 1.000\,05 r_{3\to4}$ and $r^{\mathrm{Boulder}}_{4\to3} = 0.999\,97 r_{4\to3}$, respectively, which cause the extracted value of $\mathrm{Im}(E1^{4\to3}_{\mathrm{PNC}})/\beta^{[2]}$ to decrease by 3×10^{-5} while $\mathrm{Im}(E1^{3\to4}_{\mathrm{PNC}})/\beta^{[2]}$ to increase by 5×10^{-5}. Because both $\mathrm{Im}(E1^{4\to3}_{\mathrm{PNC}})/\beta^{[2]}$, and $\mathrm{Im}(E1^{3\to4}_{\mathrm{PNC}})/\beta^{[2]}$ were reported [31] at about 1.6 mV/cm, this means that the anapole contribution in our evaluation is slightly smaller, by about $\sim1\times10^{-4}$ mV/cm. The reported [31] value of the anapole moment is 0.077(11) mV/cm so our correction of 1×10^{-4} mV/cm is below the uncertainty. This suggests that the impact due to the spin-dependent effects on polarizabilities is negligible at the current level of experimental uncertainty.

B. The effect of hyperfine-mediated polarizabilities on the α/β ratio analysis

We now turn our attention to the another Boulder experiment [30] which used the Stark-interference technique to determine the ratio of scalar and vector polarizabilities β/α in Cs.[3] This measured ratio is important in deducing the value of β through the more computationally reliable determination of α (see, e.g., Ref. [6] and the references therein). An accurate value of β is required for extracting the PNC amplitude from the APV measurement as described in Sec. V A.

In the β/α experiment [30], the ^{133}Cs atoms were spin polarized by an external magnetic field aligned along the y axis. This magnetic field defined the quantization axis that is different from that of the APV experiment described in Sec. V A. To simplify our analysis, we thus define a coordinate system (x', y', z') obtained by a rotation from the (x, y, z) laboratory frame defined in Sec. V A. The unit vectors in this system are related to those in the frame in Sec. V A as follows: $\hat{\boldsymbol{z}}' = \hat{\boldsymbol{y}}$, $\hat{\boldsymbol{y}}' = \hat{\boldsymbol{x}}$, and $\hat{\boldsymbol{x}}' = \hat{\boldsymbol{z}}$. This transformation aligns the quantization axis with $\hat{\boldsymbol{z}}'$ while preserving the handedness of the coordinate system. As a result, the electric fields in this reference frame are given by $\boldsymbol{\mathcal{E}}'_S = \mathcal{E}^x_S\hat{\boldsymbol{y}}'$ and $\boldsymbol{\mathcal{E}}'_L = \mathcal{E}^z_L\hat{\boldsymbol{x}}' + i\mathcal{E}^I_L\hat{\boldsymbol{y}}'$.

The ^{133}Cs atoms in the α/β experiment [30] underwent transitions from the initial $6S_{1/2}$, $F_i = 3$, $M_i = 3$ state to the final $7S_{1/2}$, $F_f = 3$, $M_f = 3$ state. This particular choice of states guarantees a nonvanishing contribution of the scalar polarizability to the Stark-induced amplitude, Eq. (24). Then for the described experimental geometry, one has

$$A^{\mathrm{Stark}}_{i\to f} = i\alpha^{3\to3}\,\mathcal{E}^I_L\mathcal{E}^x_S + i\beta^{3\to3}\,\mathcal{E}^x_S\mathcal{E}^z_L C^{F_f,F_i}_{M_f,M_i} + iK\,\gamma^{3\to3}\mathcal{E}^x_S\mathcal{E}^I_L, \tag{40}$$

where $K \equiv -iw_2(\hat{\boldsymbol{\epsilon}},\hat{\boldsymbol{e}})\langle F_f = 3||\{I\otimes I^{(2)}\}||F_i = 3\rangle$. Explicitly, since $\langle F_f = 3||\{I\otimes I\}^{(2)}||F_i = 3\rangle = -42\sqrt{35}$ [see

[3] We note in passing that the authors of Ref. [30] refer to β as a "tensor" polarizability, while we call it "vector" to be consistent with the literature and to distinguish it from the true tensor γ contribution.

Eq. (8)] and $w_2(\hat{\boldsymbol{\epsilon}}, \hat{\boldsymbol{\epsilon}}) = -(i/6)\sqrt{5/14}$, $K = 35/\sqrt{2}$. Here, the angular coefficient $C^{F_f F_i}_{M_f M_i}$ is defined as $C^{F_f F_i}_{M_f M_i} = g_F \langle M_F \rangle$ with the gyromagnetic ratio $g_F = -1/4$ and $\langle M_F \rangle$ being a population average over all the possible magnetic quantum numbers [30].

In contrast to the APV experiment of Sec. V A, the parity reversal in the α/β experiment was effected by switching the laser polarization from the left to right elliptical polarization, which is equivalent to reversing the sign of the $\mathcal{E}^I_L$ in Eq. (40). This reversal flips the sign of the scalar and tensor contributions, while preserving the sign of the vector term in Eq. (40). It is clear that the interference term extracted in the experiment contains the combination $(\alpha^{3\to3} + K\gamma^{3\to3})\beta^{3\to3}$. This means that we need to interpret

$$\frac{\alpha}{\beta} \to \left(\frac{\alpha}{\beta}\right)_{\text{eff}} = \frac{\alpha^{3\to3} + K\gamma^{3\to3}}{\beta^{3\to3}}, \tag{41}$$

as being the ratio measured by Ref. [30].

To prove Eq. (41), we recall that the experiment [30] employed a complementary modulation of the dc electric field strength synchronous with the elliptical polarization reversals. Two Stark-induced rates were measured,

$$R^+ = \left|\alpha^{3\to3}\mathcal{E}^I_L + \beta^{3\to3}\mathcal{E}^z_L C^{F_f F_i}_{M_f M_i} + K\gamma^{3\to3}\mathcal{E}^I_L\right|^2 \left(\mathcal{E}^x_{S,1}\right)^2, \tag{42a}$$

$$R^- = \left|\alpha^{3\to3}\mathcal{E}^I_L - \beta^{3\to3}\mathcal{E}^z_L C^{F_f F_i}_{M_f M_i} + K\gamma^{3\to3}\mathcal{E}^I_L\right|^2 \left(\mathcal{E}^x_{S,2}\right)^2, \tag{42b}$$

where $\mathcal{E}^x_{S,1}$ and $\mathcal{E}^x_{S,2}$ stand for the magnitudes of the two dc electric fields, whereas $\mathcal{E}^z_L$ and $\mathcal{E}^I_L \equiv \text{Im}(\mathcal{E}^x_L)$ are the magnitudes of the two components of the laser field driving the transition. The fields $\mathcal{E}^x_{S,1}$ and $\mathcal{E}^x_{S,2}$ were adjusted until there was no modulation of the rate signal under reversals of the laser field's polarization. This amounts to equating the two rates in Eqs. (42), thus leading to

$$\frac{\mathcal{E}^x_{S,2} - \mathcal{E}^x_{S,1}}{\mathcal{E}^x_{S,2} + \mathcal{E}^x_{S,1}} = \frac{\beta^{3\to3}}{\alpha^{3\to3} + K\gamma^{3\to3}} \frac{\mathcal{E}^z_L}{\mathcal{E}^I_L} C^{F_f F_i}_{M_f M_i}. \tag{43}$$

The inverse of the first factor on the right-hand side (rhs) of Eq. (41) was extracted using the above equation and identified as α/β in Ref. [30]. As mentioned above, the measured quantity is in fact $(\alpha/\beta)_{\text{eff}} = (\alpha^{3\to3} + K\gamma^{3\to3})/\beta^{3\to3}$.

To the best of our knowledge, all the previous literature has identified the measured [30] α/β ratio with $\alpha^{[2]}/\beta^{[2]}$, neglecting the hyperfine corrections to transition polarizabilities. We extract this ratio from the measured value [30] $(\alpha/\beta)_{\text{eff}} = -9.905(11)$ as

$$\frac{\alpha^{[2]}}{\beta^{[2]}} \approx \left(\frac{\alpha}{\beta}\right)_{\text{eff}} \left(1 - \frac{\delta\alpha^{3\to3}}{\alpha^{[2]}} - \frac{K\gamma^{3\to3}}{\alpha^{[2]}} + \frac{\delta\beta^{3\to3}}{\beta^{[2]}}\right). \tag{44}$$

With the recommended values of $\alpha^{[2]}$ and $\beta^{[2]}$ as in Eqs. (10) and the hyperfine corrections from Table I, the corrective factor on the rhs of Eq. (44) evaluates to $(1 + 1.3 \times 10^{-4})$, equivalent to a $\sim$0.01% fractional correction to the value of $\frac{\alpha^{[2]}}{\beta^{[2]}}$. The inclusion of the hyperfine correction thus modifies the last significant digit of the reported result, leading to

$$\frac{\alpha^{[2]}}{\beta^{[2]}} = -9.906(11), \tag{45}$$

but is below the 0.1% accuracy of the experiment [30].

VI. CONCLUSION

In summary, we have introduced and evaluated the hyperfine corrections to the polarizabilities, which include the nonvanishing tensor transition polarizability γ. These HFI-mediated effects lead to a slightly smaller anapole moment extracted from the measurements of atomic parity violation by the Boulder group [2,31]. However, our computed correction is insufficient to resolve the tension with the nuclear-physics interpretation and data. We also showed that the effects of the tensor transition polarizability γ and hyperfine corrections to the scalar, α, and vector, β, transition polarizabilities are minor but not negligible for the determination of the α/β ratio from the measurements [30]. As the accuracy of experiments improves, our analysis should prove useful for interpretation of future measurements.

ACKNOWLEDGMENTS

This work was supported in part by the U.S. National Science Foundation Grants No. PHY-1912465 and No. PHY-2207546, by the Sara Louise Hartman endowed professorship in Physics, and by the Center for Fundamental Physics at Northwestern University.

[1] M. C. Noecker, B. P. Masterson, and C. E. Wieman, Phys. Rev. Lett. **61**, 310 (1988).
[2] C. S. Wood, S. C. Bennett, D. Cho, B. P. Masterson, J. L. Roberts, C. E. Tanner, and C. E. Wieman, Science **275**, 1759 (1997).
[3] W. C. Haxton and C. E. Wieman, Annu. Rev. Nucl. Part. Sci. **51**, 261 (2001).
[4] B. Desplanques, J. F. Donoghue, and B. R. Holstein, Ann. Phys. **124**, 449 (1980).
[5] M. A. Bouchiat and C. Bouchiat, J. Phys. France **36**, 493 (1975).
[6] H. B. Tran Tan, D. Xiao, and A. Derevianko, Phys. Rev. A **108**, 022808 (2023).
[7] D. A. Varshalovich, A. N. Moskalev, and V. K. Khersonskii, *Quantum Theory of Angular Momentum* (World Scientific, Singapore, 1988).
[8] V. A. Dzuba, V. V. Flambaum, and O. P. Sushkov, Phys. Rev. A **56**, R4357 (1997).
[9] M. S. Safronova, W. R. Johnson, and A. Derevianko, Phys. Rev. A **60**, 4476 (1999).
[10] A. A. Vasilyev, I. M. Savukov, M. S. Safronova, and H. G. Berry, Phys. Rev. A **66**, 020101(R) (2002).
[11] V. A. Dzuba, V. V. Flambaum, and J. S. M. Ginges, Phys. Rev. D **66**, 076013 (2002).

[12] G. Toh, A. Damitz, C. E. Tanner, W. R. Johnson, and D. S. Elliott, Phys. Rev. Lett. **123**, 073002 (2019).
[13] S. C. Bennett and C. E. Wieman, Phys. Rev. Lett. **82**, 2484 (1999).
[14] V. A. Dzuba and V. V. Flambaum, Phys. Rev. A **62**, 052101 (2000).
[15] B. K. Sahoo and B. P. Das, arXiv:2008.08941.
[16] K. Beloy, U. I. Safronova, and A. Derevianko, Phys. Rev. Lett. **97**, 040801 (2006).
[17] V. A. Dzuba, V. V. Flambaum, K. Beloy, and A. Derevianko, Phys. Rev. A **82**, 062513 (2010).
[18] P. Rosenbusch, S. Ghezali, V. A. Dzuba, V. V. Flambaum, K. Beloy, and A. Derevianko, Phys. Rev. A **79**, 013404 (2009).
[19] D. DeMille and M. Kozlov, arXiv:physics/9801034.
[20] W. R. Johnson, *Atomic Structure Theory: Lectures on Atomic Physics* (Springer, New York, 2007).
[21] V. Gerginov, A. Derevianko, and C. E. Tanner, Phys. Rev. Lett. **91**, 072501 (2003).
[22] D. Das and V. Natarajan, J. Phys. B: At., Mol. Opt. Phys. **41**, 035001 (2008).
[23] H. B. Tran Tan and A. Derevianko, Phys. Rev. A **107**, 042809 (2023).
[24] K. Beloy and A. Derevianko, Comput. Phys. Commun. **179**, 310 (2008).
[25] A. Kramida, Y. Ralchenko, and J. Reader, NIST Atomic Spectra Database, https://physics.nist.gov/asd.
[26] G. Belin, L. Holmgren, and S. Svanberg, Phys. Scr. **14**, 39 (1976).
[27] E. Arimondo, M. Inguscio, and P. Violino, Rev. Mod. Phys. **49**, 31 (1977).
[28] M. Auzinsh, K. Bluss, R. Ferber, F. Gahbauer, A. Jarmola, M. S. Safronova, U. I. Safronova, and M. Tamanis, Phys. Rev. A **75**, 022502 (2007).
[29] A. Derevianko, M. S. Safronova, and W. R. Johnson, Phys. Rev. A **60**, R1741(R) (1999).
[30] D. Cho, C. S. Wood, S. C. Bennett, J. L. Roberts, and C. E. Wieman, Phys. Rev. A **55**, 1007 (1997).
[31] C. S. Wood, S. C. Bennett, J. L. Roberts, D. Cho, and C. E. Wieman, Can. J. Phys. **77**, 7 (1999).
[32] S. L. Gilbert and C. E. Wieman, Phys. Rev. A **34**, 792 (1986).